

1 The retreat pattern of glaciers controls the occurrence of turbidity currents on  
2 high-latitude fjord deltas

3 **A. Normandeau<sup>1</sup>, P. Dietrich<sup>2</sup>, J. Hughes Clarke<sup>3</sup>, W. Van Wychen<sup>4</sup>, P. Lajeunesse<sup>5</sup>, D.**  
4 **Burgess<sup>6</sup>, J-F. Ghienne<sup>7</sup>,**

5 <sup>1</sup> Geological Survey of Canada (Atlantic), Natural Resources Canada, Dartmouth, Nova  
6 Scotia, B2Y 4A2, Canada

7 <sup>2</sup> Department of Geology, Auckland Park Kingsway Campus, University of Johannesburg,  
8 Johannesburg, South Africa

9 <sup>3</sup> Center for Coastal and Ocean Mapping, University of New Hampshire, 24 Colovos Road,  
10 Durham, New Hampshire 03824, USA

11 <sup>4</sup> Defense Research and Development Canada, Department of National Defense, Ottawa,  
12 Canada.

13 <sup>5</sup> Centre d'Études Nordiques & Département de Géographie, Université Laval, 2405 Rue de la  
14 Terrasse, Québec, Québec G1V 0A6, Canada

15 <sup>6</sup> Natural Resources Canada, Geological Survey of Canada, 601 Booth St., Ottawa, ON K1A  
16 0E8, Canada

17 <sup>7</sup> Institut de Physique du Globe de Strasbourg, UMR 7516 CNRS/Université de Strasbourg, 1  
18 rue Blessig, 67084 Strasbourg, France

19

20 Corresponding author: Alexandre Normandeau ([alexandre.normandeau@canada.ca](mailto:alexandre.normandeau@canada.ca))

21

## 22 **Key points:**

- 23 • Glacial erosion is necessary to provide the sediment supply required for turbidity  
24 currents to be generated on delta fronts
- 25 • Lakes formed during glacial retreat significantly alter sediment delivery, stopping  
26 turbidity currents
- 27 • Pattern of retreating glaciers dictates the non-linear nearshore hydrodynamics of fjords

## 28 **Abstract**

29 Glacier and ice sheet mass loss as a result of climate change is driving important coastal changes  
30 in Arctic fjords. Yet, limited information exists for Arctic coasts regarding the influence of  
31 glacial erosion and ice mass loss on the occurrence and character of turbidity currents in fjords  
32 which themselves affect delta dynamics. Here, we show how glacial erosion and the production  
33 of meltwaters and sediments associated with the melting of retreating glaciers control the  
34 generation of turbidity currents in fjords of eastern Baffin Island (Canada). The subaqueous  
35 parts of 31 river mouths were mapped by high-resolution swath bathymetry along eastern Baffin  
36 Island in order to assess the presence or absence of sediment waves formed by turbidity currents  
37 on delta fronts. By extracting glaciological and hydrological watershed characteristics of these  
38 river mouths, we demonstrate that the presence and areal extent of glaciers is a key control for  
39 generating turbidity currents in fjords. However, lakes formed upstream during glacial retreat  
40 significantly alter the course of sediment routing to the deltas by forming temporary sinks,  
41 leading to the cessation of turbidity currents in the fjords. Due to the different deglaciation  
42 stages of watersheds in eastern Baffin Island, we put these results into a temporal framework  
43 of watershed deglaciation to demonstrate how the retreat pattern of glaciers, through the  
44 formation and filling of proglacial lakes, affects the activity of deltas.

## 45 **1 Introduction**

46 High-latitude coasts are particularly sensitive to a warming climate which promotes ice mass  
47 loss (Gardner et al., 2011; Zwally et al., 2011), longer open sea-ice seasons (Overeem et al.,  
48 2011; Serreze et al., 2007) and, in some regions, a relative sea-level rise (e.g., Ford et al., 2018).  
49 These environmental changes in turn drastically modify Arctic coastlines, either by increasing  
50 coastal erosion (e.g., Lantuit & Pollard, 2008), or conversely, by promoting rapid progradation  
51 of deltas due to glacial ice mass loss (e.g., Bendixen et al., 2017). Fjord-head deltas constitute  
52 the main transition zones where sediment, fossil and modern organic carbon (Galy et al., 2008;  
53 Smith et al., 2015) and contaminants (e.g., Perner et al., 2010) transit to reach deeper marine  
54 environments through river-generated density flows such as turbidity currents. Hence, rapid  
55 changes in coastal dynamics have a direct impact on these fluxes and strongly affect the  
56 nearshore environment and other associated processes in the deeper segments of the fjords, such  
57 as sediment distribution, benthos development (Syvitski et al., 1989), or the burial of organic  
58 carbon, which plays a crucial role in controlling O<sub>2</sub> and CO<sub>2</sub> concentrations (Smith et al., 2015).

59 Despite the importance of turbidity currents in the transfer of sediment and carbon to deeper-  
60 water ecosystems (Biscara et al., 2011), remarkably little information exists on sediment  
61 transport processes on high-latitude deltas due to a lack of high-resolution bathymetric data and  
62 in-situ monitoring. In the eastern Baffin Island region (Canada) (Fig. 1), the links between the  
63 pattern of ongoing glacial retreat (Lenaerts et al., 2013) and sediment transport to the coast  
64 provide a complete understanding of the consequences of deglaciation on sediment fluxes and  
65 partitioning in fjord systems. Therefore, the factors responsible for the presence of turbidity  
66 currents during deglaciation can be precisely identified.

67 The effect of deglaciation on the progradation and activity of deltas is often limited to the  
68 stratigraphic record since these processes occur over hundreds to thousands of years (Dietrich  
69 et al., 2018; Winsemann et al., 2018). Therefore, the effect of the retreat pattern of glaciers on  
70 the deltaic processes are often based on outcrop studies or from the interpretation of sediment  
71 cores. Eastern Baffin Island, like many other Arctic and Antarctic regions (e.g., Velicogna,  
72 2009), is experiencing ongoing glacial retreat, and presents a complete range of deglaciation  
73 stages: from marine terminating glaciers to complete retreat from watersheds. These different  
74 settings allow us to understand variations in sediment supply and its effect on deltaic  
75 progradation and the occurrence of turbidity currents. These variations can then be  
76 conceptualized into a temporal framework, from fully glacierized watersheds to their complete  
77 deglaciation. The modern environments of eastern Baffin Island allow us to not only understand  
78 the factors controlling the occurrence of turbidity currents but also the effect of the retreat  
79 pattern of glaciers on deltaic activity.

80 Here we present the results of extensive mapping of the submarine geomorphology of 31 fjord  
81 river mouths using high-resolution ( $\leq 5$  m) multibeam bathymetry data and characterize their  
82 relationship to glaciological and hydrological components of their watershed. The objectives of  
83 this study are threefold. First, the linkages between submarine sedimentary processes and the  
84 glaciological and hydrological components of watersheds allows to precise the factors  
85 controlling the occurrence of turbidity current on fjord deltas. Second, the different stages of  
86 deglaciation between watersheds allow us to build a temporal framework for the effect of the  
87 retreat pattern of glaciers on deltaic activity and the occurrence of turbidity currents. Thirdly,  
88 based on the established controls over turbidity currents occurrence, we can predict where these  
89 processes are likely to be active for the entire eastern Baffin Island fjords and speculate on  
90 future trends. Our findings have implications for the interpretation of past (Holocene and older)

91 deglaciation sequences and for the assessment of coastal dynamics of areas affected by glacial  
92 retreat worldwide.

## 93 **2 Material and methods**

### 94 2.1 Datasets

95 This study is based on the analysis of bathymetric datasets collected on the Research Vessel  
96 (RV) Nuliajuk in 2012-2014 and the Canadian Coast Guard Ship (CCGS) Amundsen between  
97 2006 and 2014. The multibeam bathymetric data were processed at a <5 m resolution in order  
98 to clearly visualize the presence or absence of sediment waves on delta fronts. Thirty-one deltas  
99 and river mouths were mapped in this manner along the fjords of eastern Baffin Bay (Fig. 1)  
100 (e.g., Hughes-Clarke et al., 2015).

101 For each delta, watersheds were created using watershed analysis tools in ArcGIS and using the  
102 Baffin Island digital elevation model (DEM; 25 m horizontal resolution) from the Canadian  
103 Digital Elevation Model (CDEM) (Fig. 2). Rivers were classified using the Strahler  
104 classification and a threshold of 100 pixel was used to define a class 1 river (Fig. 2F).

105 For each watershed, glaciological and hydrological characteristics were extracted using zonal  
106 statistics in ArcGIS (Fig. 2). The areas (m<sup>2</sup>) of the watersheds were calculated along with glacial  
107 ice areas, from Randolph Glacier Inventory (Pfeffer et al., 2014), and glacial ice velocity (Van  
108 Wychen et al., 2015) (m y<sup>-1</sup>). The sum of glacial ice velocity (sum of pixels) was used in this  
109 study as a proxy for glacial erosion. Pixel sizes for the ice velocity were 100 × 100 m<sup>2</sup> and the  
110 sum of the velocity for all pixels within the watershed was calculated. The ice velocity dataset  
111 covers 99% of the Randolph Glacier Inventory dataset. Two watersheds were not fully covered  
112 by the glacial ice velocity dataset and thus, this parameter was ignored for those two watersheds.  
113 Lake area was calculated using the HydroShed Global Lake Database (Messenger et al., 2016).  
114 For the 31 watersheds described in detail in this study, observation of lakes smaller than what  
115 the Global Lake Database provides were added manually. For the predictive map (see  
116 Discussion), the Global Lake Database was used without modification.

117 Watersheds were also created for all the lakes located within the fjord-delta watersheds and  
118 data extracted from these sub-watersheds were removed from the total watershed values,  
119 producing new adjusted watershed values that exclude lake sediment trapping (Fig. 2G).

### 120 2.2 Statistical analyses

121 Shapiro-Wilk normality tests and QQ normal plots were used to assess normality of  
122 distributions. Since distributions were non-normal for most of the extracted parameters, a  
123 Wilcoxon-Mann-Whitney test was used to determine if active and inactive deltas had significant  
124 differences in watershed characteristic. This non-parametric test was used to test differences  
125 between two conditions (active vs inactive deltas) and glaciological and hydrological  
126 characteristics of watersheds (presence of glacial ice, ice velocity, river classification, etc.). The  
127 test was done using the independent Wilcoxon's rank-sum test in R, which is equivalent to the  
128 Mann-Whitney test. A p-value  $< 0.05$  indicates a statistical difference between the two  
129 distributions (active and inactive deltas). In most instances, ties in the datasets were present and  
130 thus, the values were slightly modified (using *jitter* in R) in order to compute exact p-values.  
131 An effect size was then calculated in R to estimate the size of the effect observed following  
132 Field et al. (2012).

133 In addition to a Wilcoxon-Mann-Whitney test, the homogeneity of variance of the active and  
134 inactive deltas glaciological and hydrological parameters were compared. Since normal  
135 distributions could not be assumed for all datasets, a Fligner-Killeen test was used instead of  
136 the more common F-test. A p-value  $< 0.05$  indicates a significant difference in variance between  
137 the two conditions.

### 138 **3 Approach: Sediment waves as indicators of deltaic activity**

139 The main terrestrial parameter driving nearshore fjord hydrodynamics is river inflow, which  
140 controls submarine delta activity by generating turbidity currents (Syvitski, 1989; Hughes  
141 Clarke, 2016). Submarine delta activity is here viewed through the prism of subaqueous  
142 sediment wave organization. In this study, submarine delta activity is therefore defined as the  
143 presence of recurring and highly energetic turbidity currents, triggered at the delta front, and  
144 flowing downslope. These turbidity currents typically form sediment waves, the presence of  
145 which along delta slope is used to assess if a particular delta is active. In the absence of direct  
146 observations of turbidity currents, we use the absence or presence of sediment waves on delta  
147 slopes as an indicator of deltaic inactivity and activity, respectively. Sediment waves, which  
148 most of them are crescentic, are interpreted as upper-flow regime bedforms, probably cyclic  
149 steps (Cartigny et al., 2011; Hughes Clarke, 2016). Cyclic steps are sediment waves that are  
150 bounded by hydraulic jumps and that migrate upstream (Kostic et al., 2010). These types of  
151 sediment waves are known to be present on active delta slopes (Fricke et al., 2015; Clare et al.,  
152 2016; Hughes Clarke, 2016; Normandeau et al., 2016) and to be formed by high-density

153 turbidity currents (Cartigny et al., 2011); their presence indicates active processes (e.g., Smith  
154 et al., 2005; Normandeau et al., 2014).

155 Repeat bathymetric surveys of three submarine deltas in Oliver Sound (northeast Baffin Island)  
156 in 2006 and 2008 and of Southwind fjord between 2013 and 2018 shows that sediment waves  
157 migrated over these two-year periods (Fig. 3). Figure 3A-G shows the morphology of two delta  
158 fronts in 2006 and 2008 along with the differences in bathymetry between the two years. These  
159 data clearly show that the sediment waves have migrated between the two years and that channel  
160 erosion occurred. These seafloor changes confirm that the presence of sediment waves indicates  
161 recurring turbidity currents, and therefore, active submarine deltas. These types of sediment  
162 waves and seafloor changes are known to be the effect of turbidity currents (Corella et al., 2014;  
163 Fricke et al., 2015; Normandeau et al., 2016; Hage et al., 2018) and cannot be attributed to  
164 oceanographic processes. The absence of sediment waves conversely indicates that the deltas  
165 are no longer active and that turbidity currents do not occur.

## 166 **4 Results**

### 167 4.1 Glaciological and hydrological parameters of active and inactive deltas

168 High-resolution multibeam bathymetric imagery available for 31 river mouths and deltas reveal  
169 16 active and 15 inactive deltas (Fig. 1). The median percentage of glacial ice in watersheds of  
170 active deltas is 50% ( $Q_1=37\%$ ,  $Q_3=60\%$ ) compared to 22% ( $Q_1=14\%$ ,  $Q_3=31\%$ ) for inactive  
171 ones (Fig. 4G). In order to assess if active and inactive deltas have significantly different  
172 glaciological and hydrological settings in their watershed, a non-parametric Wilcoxon-Mann-  
173 Whitney test was used. The percentage of glacial ice in the watershed is a critical factor  
174 controlling the nearshore presence of turbidity currents in fjords ( $P < 0.001$ ,  $r = 0.75$ ) (Table  
175 1, Fig. 4G). Watersheds devoid of glacial ice all have inactive deltas whereas watersheds with  
176 glacial ice can be active or inactive depending on past pattern of retreating glacier. Some  
177 inactive deltas have comparable percentage of glacial ice in their watershed to active ones (Fig.  
178 4G). In order to evaluate the effectiveness of lakes in trapping sediments, lake sub-watersheds  
179 were removed from all the watersheds, which provided new adjusted watersheds (Fig. 4H) with  
180 a median percentage of glacial ice of 55% ( $Q_1=44\%$ ,  $Q_3=61\%$ ) for active deltas and 1%  
181 ( $Q_1=0.1\%$ ,  $Q_3=5\%$ ) for inactive ones. When excluding the sub-watersheds that flow into lakes  
182 from delta watersheds, active deltas have watersheds with significantly more glacial ice than  
183 inactive deltas ( $P < 0.001$ ,  $r = 0.87$ ) (Table 1; Fig. 4H). The percentage of glacial ice in the  
184 sub-watersheds of lakes explains the inactivity of the deltas with high percentage of glacial ice

185 in their total watershed (Fig. 4H). Additionally, a Fligner-Killeen test shows that there is no  
186 significant difference between the variances of glacial ice in active and inactive delta  
187 watersheds when comparing their total watershed ( $P = 0.58$ ) but that there is when comparing  
188 glacial ice in the adjusted watershed ( $P = 0.03$ ) (Table 1). This significant difference between  
189 the variances indicates that watersheds of active deltas have higher variance of glacial ice than  
190 the inactive deltas, as expressed in Figure 4H where the percentage of glacial ice in adjusted  
191 watersheds for inactive deltas largely remains below 10%, but varies between 30-90% for active  
192 deltas. Furthermore, glacial ice velocity within adjusted watersheds (Fig. 4J), which is a proxy  
193 for glacial erosion (Overeem et al., 2017), is significantly higher in active delta watersheds than  
194 in inactive ones ( $P < 0.001$ ,  $r = 0.83$ ). Other parameters such as river classification ( $P = 0.11$ ,  
195  $r = 0.29$ ) (Fig. 4A), which is a proxy for river discharge (Strahler, 1957), or area of watershed  
196 ( $P = 0.21$ ,  $r = 0.22$ ) (Fig. 4B), show no significant differences between the active and inactive  
197 delta watersheds (Table 1). The area of adjusted watershed becomes, however, a significant  
198 parameter ( $P = 0.0036$ ,  $r = 0.52$ ) (Fig. 4C) because, in some cases where lakes are formed near  
199 the river mouth, the watershed area is diminished by 95% when excluding lake sub-watersheds.

## 200 **5 Discussion**

### 201 5.1 Factors controlling the occurrence of turbidity currents

202 This study demonstrates the different glaciological and hydrological parameters having an  
203 effect on the occurrence of turbidity currents on fjord deltas. Recent studies have shown that  
204 the watershed area and river discharge control the type of deltas created, i.e., small gilbert type  
205 deltas or deltas with long-running channels (Gales et al., 2018). However, our results show no  
206 significant differences between small and large watersheds on the occurrence of turbidity  
207 currents. Similarly, river classification, which is used as a proxy for river discharge, does not  
208 affect the occurrence of turbidity current at river mouths, although it may affect the  
209 development of submarine channels (Gales et al., 2018). Conversely, the presence of glaciers  
210 in the watersheds exerts a significant control over the occurrence of turbidity currents, which  
211 indicates that the presence of glaciers is critical for the supply of sediment to deltas. Glacial ice  
212 area and percentage of glacial ice are both important for the occurrence of turbidity currents.  
213 The percentage of glacial ice in the watershed exerts however a slightly stronger influence,  
214 likely because it provides an estimation of the proximity of the source of sediment (i.e., glacial  
215 erosion): higher percentage of glacial ice covers a larger area of the watershed, thereby  
216 providing a source of sediment close to the delta. A closer source of sediment reduces the

217 likelihood of sediment storage within the watershed. Conversely, small glacial ice percentage  
218 are more likely to indicate a source of glacial erosion farther upstream in the watershed, thereby  
219 increasing the likelihood of watershed sediment storage.

220 The differences between total and adjusted watersheds clearly show the influence of lakes on  
221 preventing the delivery of sediment to deltas. These differences are most clearly illustrated  
222 when looking at glacial ice percentage in active and inactive delta watersheds. Active deltas all  
223 contain similar percentage of glacial ice in their total and adjusted watersheds. However,  
224 although the percentage of glacial ice mostly varies between 14 and 31% in inactive delta  
225 watersheds, it drastically drops to 0-5% in the adjusted watersheds. A similar trend is observed  
226 when examining the glacial ice velocity –proxy for glacial erosion– since both parameters are  
227 linked. These values clearly show that lakes are efficient in trapping sediment and preventing  
228 the formation of turbidity currents on the fjord deltas. The proximity of the ice margin to the  
229 delta hence reduces the likelihood for sediment to encounter and then being trapped in a lake.

## 230 5.2 The retreat pattern of glaciers controls the occurrence of turbidity currents

231 The different deglaciation stages of the watersheds of Baffin Island allow us to better  
232 understand temporal trends in the evolution of deltas in glaciated settings and provide a  
233 conceptual model for the occurrence of turbidity currents in high-latitude environments. Some  
234 watersheds are almost fully glacierized whereas others are completely deglaciated. Examining  
235 the differences in deltaic processes and activity for this wide range of glacierized settings allows  
236 us to understand the temporal variations in sediment supply and propose a model for the  
237 evolution of a single delta/watershed during the retreat of glaciers (Fig. 5). This model begins  
238 when ice-margins become land-based and ends when ice-margins have completely retreated  
239 from the watershed.

240 The results presented here clearly demonstrate the critical role played by glacial erosion and  
241 the retreat pattern of glaciers across watersheds in modifying the type of sediment supply to  
242 fjords (Fig. 5). The supply of sediment from glacial erosion is assumed to remain relatively  
243 constant during glacier retreat (Fig 5A), as suggested by the presence of turbidity currents on  
244 deltas with watersheds comprising from 30% to 90% glacial ice. Glacial erosion provides large  
245 volumes of sediment when there is a direct connection between glacier and fjord-delta, which  
246 allows turbidity currents to form. However, during the retreat of the glaciers, proglacial lakes  
247 can form because of moraine damming, glacial overdeepening, isostatic flexure or structural  
248 inheritance (Carrivick & Tweed, 2013; Dietrich et al., 2017), and significantly alter the delivery



249 of sediment to the ocean. When lakes form, sediment supply to the fjord-head delta shuts down  
250 as sediment is trapped upstream in lakes, drastically modifying the hydrodynamics of the  
251 marine nearshore environment due to severe sediment starvation (Fig. 5A, C). Both small and  
252 large lakes act the same way in trapping sediment upstream of the delta. Sediment starvation is  
253 not due to reduced sediment supply from the glaciers but is due to sediment not reaching the  
254 coast. Because of sediment starvation, some deltas appear to have been significantly eroded,  
255 forming bays while upstream lakes in the watershed are being filled with sediment (Fig. 5C).  
256 However, once sediment completely fills the lakes, which appears to have occurred in some  
257 watersheds (Fig. 5D), deltas can be reactivated on the long term since the course of the river  
258 down to the fjord is re-established (Fig. 5). Hence, although all sizes of lakes are efficient in  
259 trapping sediment, the size of lakes influences the time period during which sediment starvation  
260 on fjord deltas occurs. Finally, when glaciers retreat from the watersheds, there is no longer  
261 enough sediment supplied through glaciofluvial rivers to generate turbidity currents, which  
262 leads to the cessation of turbidity currents and the erosion of the deltas (Fig. 5A).

263 Recent studies have shown that delta progradation is rapid in watersheds affected by glacial ice  
264 mass loss even during relative sea-level rise (Bendixen et al., 2017), which lead us to conclude  
265 that shallow bays or shelves, in some cases formed by a drowned former delta plain and which  
266 are not prone to the formation of turbidity currents, would be quickly filled by the prograding  
267 deltas, after which turbidity currents would form in deeper environments. Therefore, the  
268 presence of a shallow bay or shelf in nearshore fjords does not preclude on the long term the  
269 formation of turbidity currents after rapid filling of the shallow nearshore environment. Possible  
270 limitations to this model nonetheless include depth of the prodelta during the transition from an  
271 inactive delta to an active one (i.e., the time it takes for deltas to fill shallow bays).

272         5.3 Can we predict the occurrence of turbidity currents from glaciological and  
273 hydrological watershed characteristics?

274 Based on the results of this study, the terrestrial glaciological and hydrological characteristics  
275 of watersheds are used to identify fjords where turbidity currents are very likely, possibly or  
276 unlikely to be presently occurring. The percentage of glacial ice within the adjusted watersheds  
277 (excluding lake sub-watersheds) proved to be the most significant parameter for the presence  
278 of turbidity currents (Table 1). Therefore, this parameter was used to predict the location of  
279 active and inactive deltas for 644 fjord deltas of eastern Baffin Island (Fig. 6) where 1) less than  
280 10% glacial ice in adjusted watershed suggests that the deltas are inactive (unlikely in Fig. 6B);

281 2) between 10 and 20% glacial ice suggests that they are possibly active (possible in Fig. 6B);  
282 and 3) more than 20% glacial ice in adjusted watersheds suggest that the deltas are active (very  
283 likely in Fig. 6B). These thresholds applied to the 31 known deltas yields a 6.5% error where  
284 two inactive deltas were mistakenly interpreted as active. In these two cases, other parameters  
285 such as moraine damming or storing of sediment within the sediment-routing system appears  
286 to play a role but could not be quantified. Using percent glacial ice in adjusted watersheds is  
287 thus a strong proxy for predicting where turbidity currents occur in high-latitude fjords.

288 Although recent studies have suggested that glacier-derived sediment flux control the  
289 progradation of deltas (Bendixen et al., 2017; Dietrich et al., 2017), our findings reveal that the  
290 pattern of glacial retreat, i.e., the formation of lake due to moraine damming or glacial  
291 overdeepening, is more important than the simple presence/absence of a glacier in the watershed  
292 on the occurrence of turbidity currents. Of the 644 fjord delta watersheds of eastern Baffin  
293 Island, 48% likely have inactive deltas, 9% have deltas that are possibly active and 43% likely  
294 have active deltas. Although 60% of the deltas have an elevated proportion of glacial ice (>10  
295 %) in their watersheds, only 52% possibly or likely have turbidity currents at their fronts  
296 because of the effect of lake trapping that prevents sediment delivery to the fjords. It is however  
297 important to note that this likelihood of the occurrence of turbidity currents (Fig. 6B) is only  
298 applicable in the modern configuration of lake distribution, which inherently evolve through  
299 time.

300 As retreat of glaciers is ongoing, the pattern of retreat may modify the future hydrological and  
301 glaciological characteristics, which will then have a direct impact on the occurrence of turbidity  
302 currents in fjords. For example, if there is a stillstand during the retreat of glaciers, it is likely  
303 to construct a frontal moraine, which will then form a moraine-dammed proglacial lake that  
304 traps sediment. Conversely, if the retreat of glaciers is continuous, the formation of a proglacial  
305 lake is less likely, allowing continuous sediment delivery to fjord-deltas. Currently, studies have  
306 shown that the retreat of glaciers and ice-mass loss has accelerated in the beginning of the 21<sup>st</sup>  
307 century due to higher summer temperatures with little change in annual precipitation (Gardner  
308 et al., 2012) and that this ice mass loss appears irreversible until the end of the century (Lenaerts  
309 et al., 2013). If this accelerated ice mass loss continues as predicted, we speculate that moraine-  
310 damned lake will be less likely to form, thus enhancing in the short term the occurrence of  
311 turbidity currents in Baffin fjords. Some lakes may be filled which will allow some deltas to be  
312 reactivated. However, if ice-mass loss continues until completely melting, the occurrence of  
313 turbidity currents will cease and will have an abrupt effect on the hydrodynamics of fjords.

314

## 6 Conclusions

315 This study used the various stages of deglaciation of eastern Baffin Island to illustrate the role  
316 of the retreat pattern of glaciers on the activity of deltas through the occurrence of turbidity  
317 currents. We show that the supply of sediment to fjords, which is necessary for the formation  
318 of turbidity currents, is controlled by glacial erosion and hampered by the presence of lakes in  
319 the sediment-routing system. Glaciers on land are a necessary condition for the erosion of  
320 bedrock and the supply of large volumes of sediment to coastal and nearshore environments  
321 whereas lakes can prevent delivery to the fjords. These factors controlling the occurrence of  
322 turbidity currents were then conceptualized in a temporal framework since eastern Baffin Island  
323 comprises watersheds which are fully glacierized to fully deglaciated. These stages of  
324 deglaciation could thus be used to demonstrate the evolution of a retreating glacier and the  
325 formation of lakes on the non-linear activity of deltas (Fig. 5). Although this study is based on  
326 the modern environment, it can be used as a way to further our understanding of the effects of  
327 late-Pleistocene/early Holocene deglaciation on fjord sedimentation and to estimate future  
328 occurrence of turbidity currents in response to climate change.

329 This conceptual model is applicable to other high- to mid-latitude, high-relief (fjord) glacierized  
330 areas where glaciers feed –or not– fjord systems, such as in Arctic and Antarctic Islands,  
331 Alaska, Patagonia and New Zealand. In addition, since the formation of lakes during glacial  
332 retreat is highly variable in space and time, the timespan of delta activity is poorly predictable.  
333 Watersheds where glaciers are retreating, which is a general trend in the Arctic due to climate  
334 change (Lenaerts et al., 2013), may develop proglacial lakes in the near future, which will  
335 suddenly shut down the fjord nearshore hydrodynamics. Once lakes are filled, deltaic  
336 sedimentary processes may become active again. The acceleration of ice-mass loss however  
337 suggest that moraine-dammed lakes are less likely to form in the future in the absence of glacial  
338 stillstands, potentially enhancing temporarily the occurrence of turbidity currents in Baffin  
339 fjords. Finally, following the retreat of the glaciers from the watersheds, sediment supply will  
340 abruptly drop due to cessation of glacial supply or rerouting of glacial sediments and meltwaters  
341 to adjacent basins. Future pattern of retreating glaciers will dictate the non-linear nearshore  
342 hydrodynamics of fjords and its impact on carbon burials and ecosystems and should be taken  
343 into account in models dealing with high-latitude fjord hydrodynamics.

344 **Acknowledgements**

345 The authors wish to thank ArcticNet for the multibeam data collection. The multibeam data  
346 collected for this study are available at <http://www.omg.unb.ca/Projects/Arctic/>. The extracted  
347 glaciological and hydrological data are available in the supplementary material. This study was  
348 funded by the Geological Survey of Canada.

## 349 **References**

350 Bendixen, M., Iversen, L. L., Bjørk, A. A., Elberling, B., Westergaard-Nielsen, A., Overeem,  
351 I., Barnhart, K.R., Khan, S.A. et al. (2017). Delta progradation in Greenland driven by  
352 increasing glacial mass loss. *Nature*, 550(7674), 101.

353 Biscara, L., Mulder, T., Martinez, P., Baudin, F., Etcheber, H., Jouanneau, J. M., & Garlan, T.  
354 (2011). Transport of terrestrial organic matter in the Ogooué deep sea turbidite system  
355 (Gabon). *Marine and Petroleum Geology*, 28(5), 1061-1072.

356 Carrivick, J. L., & Tweed, F. S. (2013). Proglacial lakes: character, behaviour and geological  
357 importance. *Quaternary Science Reviews*, 78, 34-52.

358 Cartigny, M. J., Postma, G., van den Berg, J. H., & Mastbergen, D. R. (2011). A comparative  
359 study of sediment waves and cyclic steps based on geometries, internal structures and numerical  
360 modeling. *Marine Geology*, 280(1-4), 40-56.

361 Clare, M. A., Clarke, J. H., Talling, P. J., Cartigny, M. J., & Pratomo, D. G. (2016).  
362 Preconditioning and triggering of offshore slope failures and turbidity currents revealed by most  
363 detailed monitoring yet at a fjord-head delta. *Earth and Planetary Science Letters*, 450, 208-  
364 220.

365 Corella, J. P., Arantegui, A., Loizeau, J. L., DelSontro, T., Le Dantec, N., Stark, N., ... &  
366 Girardclos, S. (2014). Sediment dynamics in the subaquatic channel of the Rhone delta (Lake  
367 Geneva, France/Switzerland). *Aquatic sciences*, 76(1), 73-87.

368 Dietrich, P., Ghienne, J. F., Normandeau, A., & Lajeunesse, P. (2017). Reconstructing ice-  
369 margin retreat using delta morphostratigraphy. *Scientific reports*, 7(1), 16936.

370 Dietrich, P., Ghienne, J. F., Lajeunesse, P., Normandeau, A., Deschamps, R., & Razin, P.  
371 (2018). Deglacial sequences and glacio-isostatic adjustment: Quaternary compared with  
372 Ordovician glaciations. *Geological Society, London, Special Publications*, 475, SP475-9.

373 Field, A., Miles, J., & Field, Z. (2012). *Discovering statistics using R*. Sage publications.

- 374 Ford, J. D., Couture, N., Bell, T., & Clark, D. G. (2017). Climate change and Canada's north  
375 coast: Research trends, progress, and future directions. *Environmental Reviews*, 26(1), 82-92.
- 376 Fricke, A. T., Sheets, B. A., Nittrouer, C. A., Allison, M. A., & Ogston, A. S. (2015). An  
377 examination of Froude-supercritical flows and cyclic steps on a subaqueous lacustrine delta,  
378 Lake Chelan, Washington, USA. *Journal of Sedimentary Research*, 85(7), 754-767.
- 379 Gales, J. A., Talling, P. J., Cartigny, M. J., Hughes Clarke, J., Lintern, G., Stacey, C., & Clare,  
380 M. A. (2018). What controls submarine channel development and the morphology of deltas  
381 entering deep-water fjords?. *Earth Surface Processes and Landforms*.
- 382 Galy, V., France-Lanord, C., & Lartiges, B. (2008). Loading and fate of particulate organic  
383 carbon from the Himalaya to the Ganga–Brahmaputra delta. *Geochimica et Cosmochimica*  
384 *Acta*, 72(7), 1767-1787.
- 385 Gardner, A., Moholdt, G., Arendt, A., & Wouters, B. (2012). Accelerated contributions of  
386 Canada's Baffin and Bylot Island glaciers to sea level rise over the past half century. *The*  
387 *Cryosphere*, 6(5), 1103.
- 388 Gardner, A. S., Moholdt, G., Wouters, B., Wolken, G. J., Burgess, D. O., Sharp, M. J., ... &  
389 Labine, C. (2011). Sharply increased mass loss from glaciers and ice caps in the Canadian  
390 Arctic Archipelago. *Nature*, 473(7347), 357.
- 391 Hage, S., Cartigny, M. J., Clare, M. A., Sumner, E. J., Vendettuoli, D., Hughes Clarke, J. E.,  
392 Hubbard, S.M., Vardy, M.E. et al. (2018). How to recognize crescentic bedforms formed by  
393 supercritical turbidity currents in the geologic record: Insights from active submarine  
394 channels. *Geology*, 46(6), 563-566.
- 395 Hughes Clarke, J. E., Muggah, J., Renoud, W., Bell, T., Forbes, D. L., Cowan, B., & Kennedy,  
396 J. (2014). Reconnaissance seabed mapping around Hall and Cumberland Peninsulas, Nunavut:  
397 Opening up southeast Baffin Island to nearshore geological investigations. *Summary of*  
398 *activities*, 133-144.
- 399 Hughes Clarke, J. E. (2016). First wide-angle view of channelized turbidity currents links  
400 migrating cyclic steps to flow characteristics. *Nature communications*, 7, 11896.
- 401 Kostic, S., Sequeiros, O., Spinewine, B., & Parker, G. (2010). Cyclic steps: A phenomenon of  
402 supercritical shallow flow from the high mountains to the bottom of the ocean. *Journal of*

403 *Hydro-environment Research*, 3(4), 167-172.

404 Lantuit, H., & Pollard, W. H. (2008). Fifty years of coastal erosion and retrogressive thaw slump  
405 activity on Herschel Island, southern Beaufort Sea, Yukon Territory,  
406 Canada. *Geomorphology*, 95(1-2), 84-102.

407 Lenaerts, J. T., van Angelen, J. H., van den Broeke, M. R., Gardner, A. S., Wouters, B., & van  
408 Meijgaard, E. (2013). Irreversible mass loss of Canadian Arctic Archipelago  
409 glaciers. *Geophysical Research Letters*, 40(5), 870-874.

410 Messenger, M. L., Lehner, B., Grill, G., Nedeva, I., & Schmitt, O. (2016). Estimating the volume  
411 and age of water stored in global lakes using a geo-statistical approach. *Nature*  
412 *communications*, 7, 13603.

413 Normandeau, A., Lajeunesse, P., St-Onge, G., Bourgault, D., Drouin, S. S. O., Senneville, S.,  
414 & Bélanger, S. (2014). Morphodynamics in sediment-starved inner-shelf submarine canyons  
415 (Lower St. Lawrence Estuary, Eastern Canada). *Marine Geology*, 357, 243-255.

416 Normandeau, A., Lajeunesse, P., Poiré, A. G., & Francus, P. (2016). Morphological expression  
417 of bedforms formed by supercritical sediment density flows on four fjord-lake deltas of the  
418 south-eastern Canadian Shield (Eastern Canada). *Sedimentology*, 63(7), 2106-2129.

419 Overeem, I., Anderson, R. S., Wobus, C. W., Clow, G. D., Urban, F. E., & Matell, N. (2011).  
420 Sea ice loss enhances wave action at the Arctic coast. *Geophysical Research Letters*, 38(17).

421 Overeem, I., Hudson, B. D., Syvitski, J. P., Mikkelsen, A. B., Hasholt, B., van den Broeke, M.  
422 R., ... & Morlighem, M. (2017). Substantial export of suspended sediment to the global oceans  
423 from glacial erosion in Greenland. *Nature Geoscience*, 10(11), ngeo3046.

424 Perner, K., Leipe, T., Dellwig, O., Kuijpers, A., Mikkelsen, N., Andersen, T. J., & Harff, J.  
425 (2010). Contamination of arctic Fjord sediments by Pb–Zn mining at Maarmorilik in central  
426 West Greenland. *Marine pollution bulletin*, 60(7), 1065-1073.

427 Pfeffer, W. T., Arendt, A. A., Bliss, A., Bolch, T., Cogley, J. G., Gardner, A. S., Hagen, J.O.,  
428 Hock, R. et al. (2014). The Randolph Glacier Inventory: a globally complete inventory of  
429 glaciers. *Journal of Glaciology*, 60(221), 537-552.

430 Serreze, M. C., Holland, M. M., & Stroeve, J. (2007). Perspectives on the Arctic's shrinking  
431 sea-ice cover. *science*, 315(5818), 1533-1536.

- 432 Smith, D. P., Ruiz, G., Kvitek, R., & Iampietro, P. J. (2005). Semiannual patterns of erosion  
433 and deposition in upper Monterey Canyon from serial multibeam bathymetry. *GSA*  
434 *Bulletin*, 117(9-10), 1123-1133.
- 435 Smith, R. W., Bianchi, T. S., Allison, M., Savage, C., & Galy, V. (2015). High rates of organic  
436 carbon burial in fjord sediments globally. *Nature Geoscience*, 8(6), ngeo2421.
- 437 Strahler, A. N. (1957). Quantitative analysis of watershed geomorphology. *Eos, Transactions*  
438 *American Geophysical Union*, 38(6), 913-920.
- 439 Syvitski, J. P. (1989). On the deposition of sediment within glacier-influenced fjords:  
440 oceanographic controls. *Marine Geology*, 85(2-4), 301-329.
- 441 Syvitski, J. P., Farrow, G. E., Atkinson, R. J. A., Moore, P. G., & Andrews, J. T. (1989). Baffin  
442 Island fjord macrobenthos: bottom communities and environmental significance. *Arctic*, 232-  
443 247.
- 444 Velicogna, I. (2009). Increasing rates of ice mass loss from the Greenland and Antarctic ice  
445 sheets revealed by GRACE. *Geophysical Research Letters*, 36(19).
- 446 Winsemann, J., Lang, J., Polom, U., Loewer, M., Igel, J., Pollok, L., & Brandes, C. (2018). Ice-  
447 marginal forced regressive deltas in glacial lake basins: geomorphology, facies variability and  
448 large-scale depositional architecture. *Boreas*.
- 449 Van Wychen, W., Copland, L., Burgess, D. O., Gray, L., & Schaffer, N. (2015). Glacier  
450 velocities and dynamic discharge from the ice masses of Baffin Island and Bylot Island,  
451 Nunavut, Canada. *Canadian Journal of Earth Sciences*, 52(11), 980-989.
- 452 Zwally, H. J., Li, J., Brenner, A. C., Beckley, M., Cornejo, H. G., DiMARZIO, J., ... & Yi, D.  
453 (2011). Greenland ice sheet mass balance: distribution of increased mass loss with climate  
454 warming; 2003–07 versus 1992–2002. *Journal of Glaciology*, 57(201), 88-102.

455 **TABLE AND FIGURE CAPTIONS**

456 **Table 1:** Factors controlling the presence of turbidity currents on fjord-deltas. A Wilcoxon-  
457 Mann-Whitney test was used to compare active vs inactive deltas. Percentage of glacial ice is  
458 the main controlling factor and statistical significance increases when taking lakes as efficient  
459 sediment traps into consideration (adjusted watersheds). The Fligner-Killeen test checks for  
460 homogeneity of variance between the distributions and indicates if the difference in variance is  
461 significant ( $p < 0.05$ ) or not.

462 **Figure 1:** Distribution of the active and inactive delta watersheds along eastern Baffin Island  
463 with bathymetric examples of inactive (A, B) and active deltas (C, D, E).

464 **Figure 2:** Method for the extraction of glaciological and hydrological data: A) Satellite image  
465 of the Pangnirtung fjord-head delta and watershed; B) Delimitation of its watershed (green  
466 line); C) Extraction of glacial ice area within the watershed; D) Extraction of glacial ice velocity  
467 within the watershed; E) Extraction of the area of lakes within the watershed; F) Extraction of  
468 river classification within the watershed; G) Delimitation of the adjusted watersheds from  
469 which the previous glaciological and hydrological characteristics were re-extracted.

470 **Figure 3:** Examples of recurring turbidity currents leading to the migration of sediment waves  
471 (cyclic steps) on two fjord-head deltas between 2006 and 2008. A) Location of Oliver Sound  
472 and the fjord-head deltas; B) Bathymetry of western Oliver Sound delta in 2006; C) Bathymetry  
473 of western Oliver Sound delta in 2008; D) Elevation difference map of western Oliver Sound  
474 between 2006 and 2008 illustrating channel erosion and the migration of sediment waves; E)  
475 Bathymetry of eastern Oliver Sound delta in 2006; C) Bathymetry of eastern Oliver Sound delta  
476 in 2008; D) Elevation difference map of eastern Oliver Sound between 2006 and 2008  
477 illustrating channel erosion and the migration of sediment waves.

478 **Figure 4:** Boxplots of the glaciological and hydrological parameters controlling turbidity  
479 currents (TC) in fjord-head deltas. River classification (A), area of watershed (B), area of  
480 adjusted watershed (C), glacial ice area (D), glacial ice area in adjusted watershed (E),  
481 percentage of lake (F), percentage of glacial ice (G), percentage of glacial ice in adjusted  
482 watershed (H), glacial ice velocity (I) and glacial ice velocity in adjusted watershed (J) were all  
483 tested against the presence or absence of sediment waves (TC or No TC). The percentage of  
484 glacial ice in adjusted watershed (H) was found to be the main controlling factor on the presence  
485 of sediment waves and therefore, on the occurrence of turbidity currents in fjords.



486 **Figure 5:** Effect of watershed characteristics on deltaic activity. A) Proposed model for the  
487 occurrence of turbidity currents during glacier retreat: 1) A direct connection between glacial  
488 erosion and the delta will lead to the occurrence of turbidity currents (B, E). 2) The presence of  
489 a lake caused by glacial retreat (e.g., by moraine damming or glacial overdeepening) will alter  
490 the delivery of sediment to the delta (C, F). 3) However, if the lake is filled, the connection will  
491 be re-established, leading to the reactivation of turbidity currents (D, G).

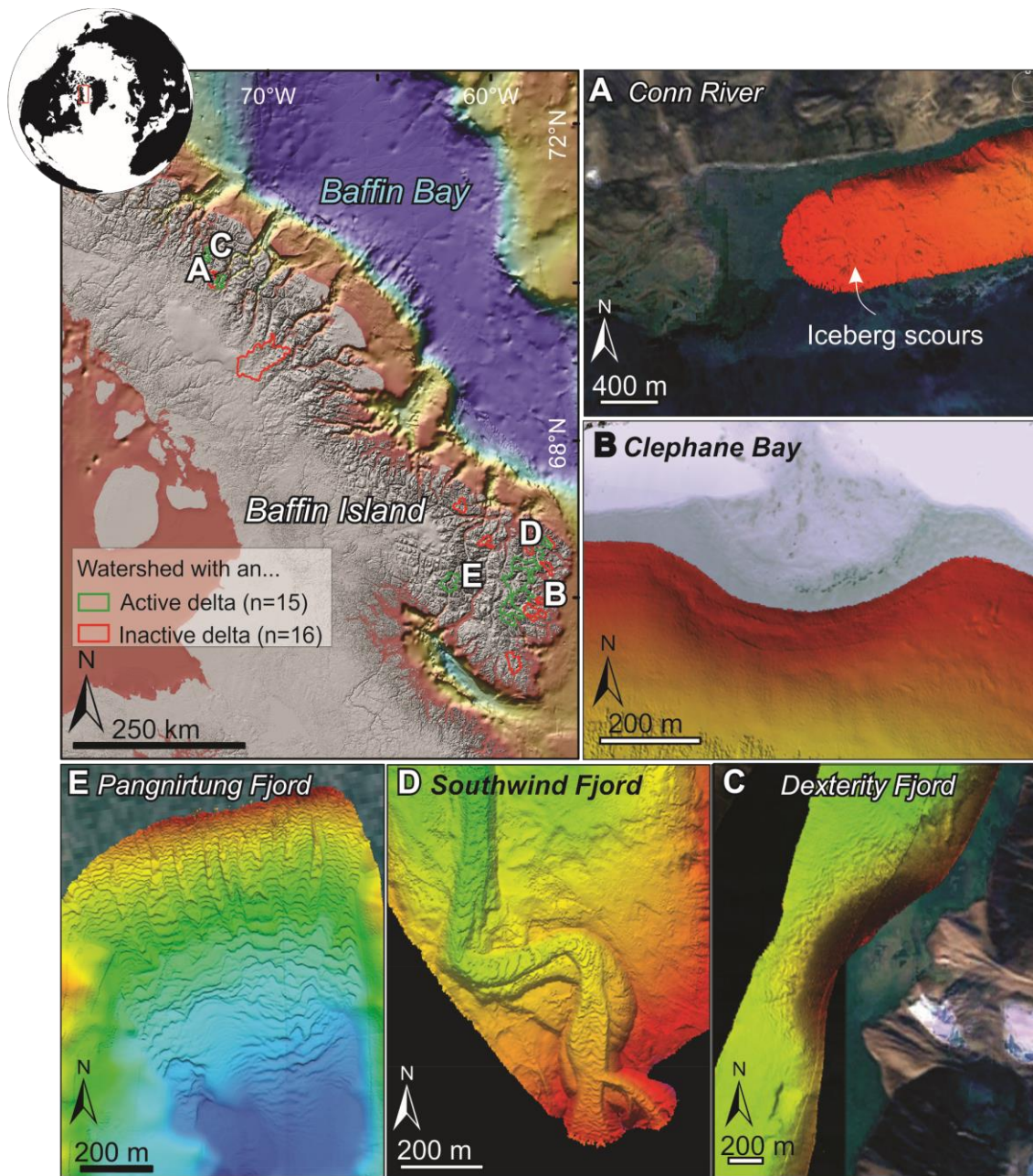
492 **Figure 6:** A) Distribution of glacial ice and glacial ice velocity in eastern Baffin Island. B)  
493 Predictive map of fjord deltas with currently occurring turbidity currents. Very likely active  
494 turbidity currents have >20% glacial ice in their adjusted watersheds (excluding lake sub-  
495 watershed). Possibly active deltas (possible in B) have 10-20% glacial ice in their adjusted  
496 watersheds. Inactive deltas (unlikely in B) have less than 10% glacial ice in their adjusted  
497 watersheds.

498 **Table 1**

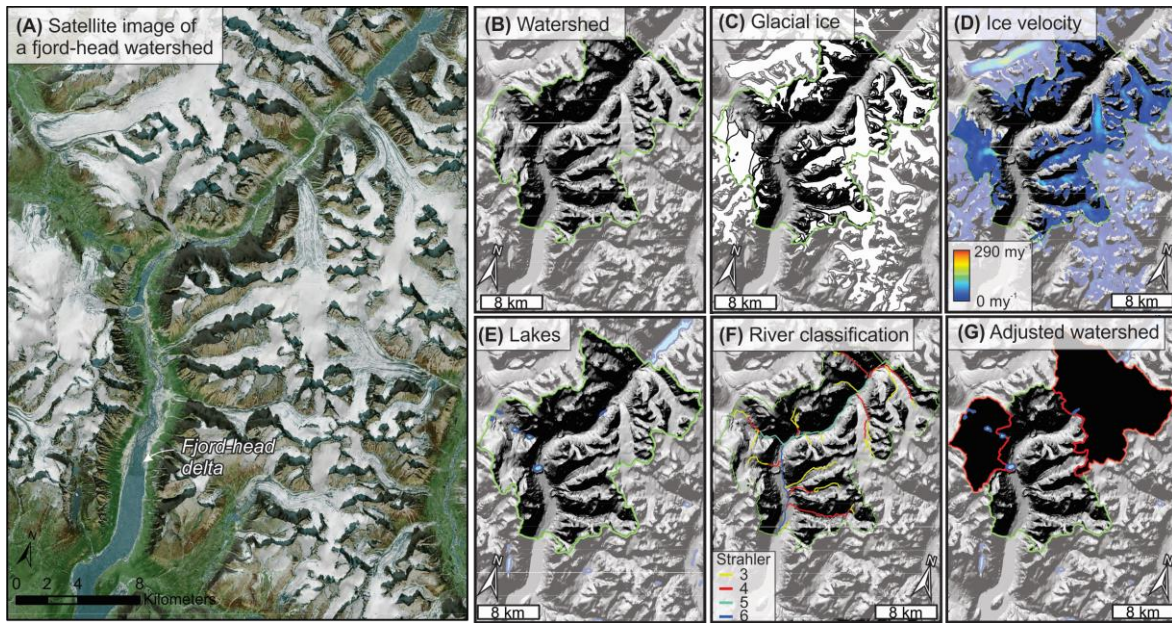
<b>Variable</b>	<b>Wilcoxon-Mann-Whitney p-value</b>	<b>Effect size (r)</b>	<b>Fligner-Killeen p-value</b>
Percentage glacial ice in adjusted watershed	0.000001	0.87	0.03
Sum of glacial ice velocity in adjusted watershed	0.000007	0.83	0.001
Glacial ice area in adjusted watershed	0.00001	0.79	0.0004
Percentage glacial ice in watershed	0.00003	0.75	0.58
Area of adjusted watershed	0.0036	0.52	0.003
Sum of glacial ice velocity in watershed	0.004	0.53	0.04
Glacial ice area in watershed	0.005	0.5	0.01
Percentage lake area in watershed	0.006	0.46	0.046
River classification (Strahler)	0.11	0.29	0.53
Area of watershed	0.21	0.22	0.14

499

500 **Figure 1**

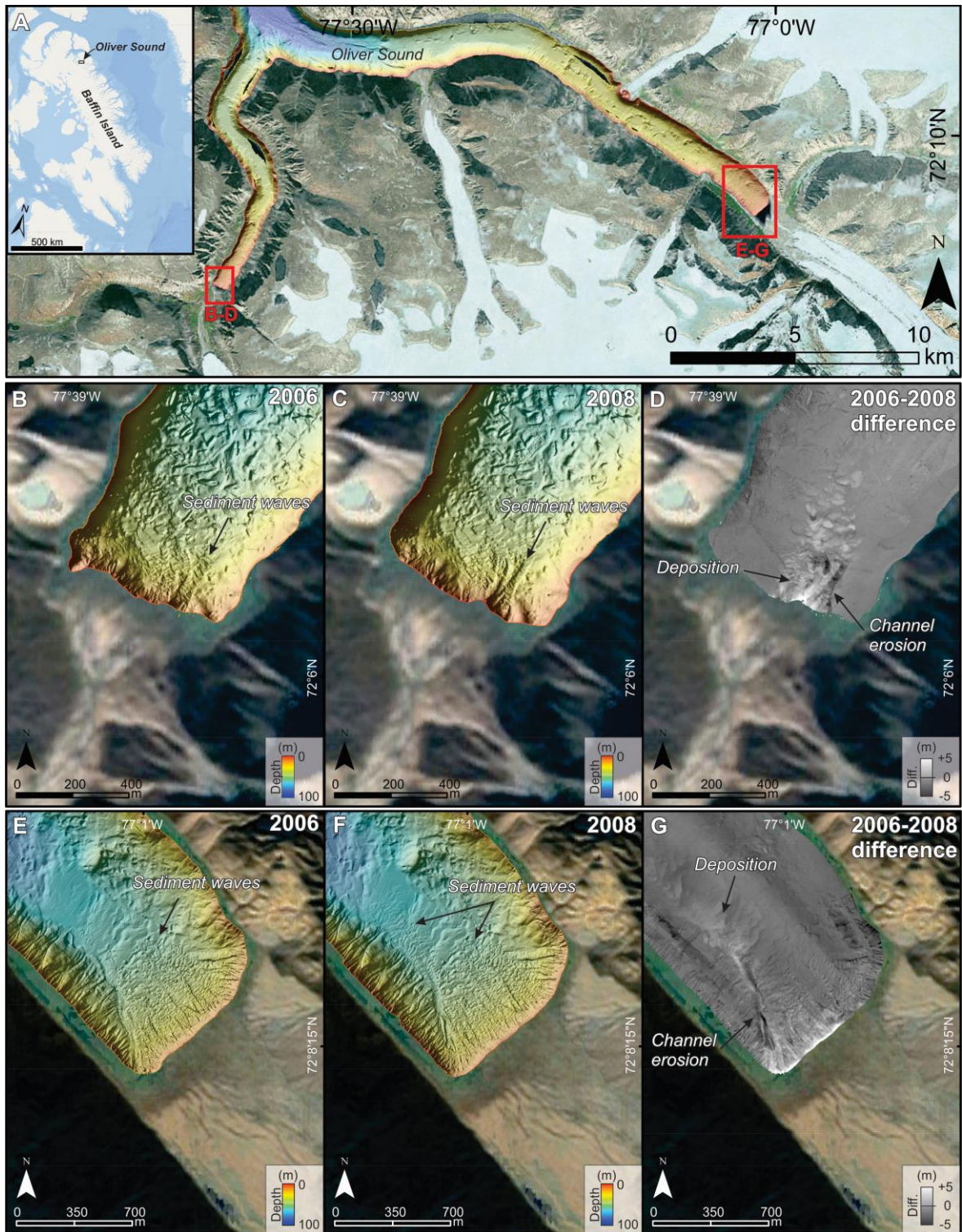


502 **Figure 2**



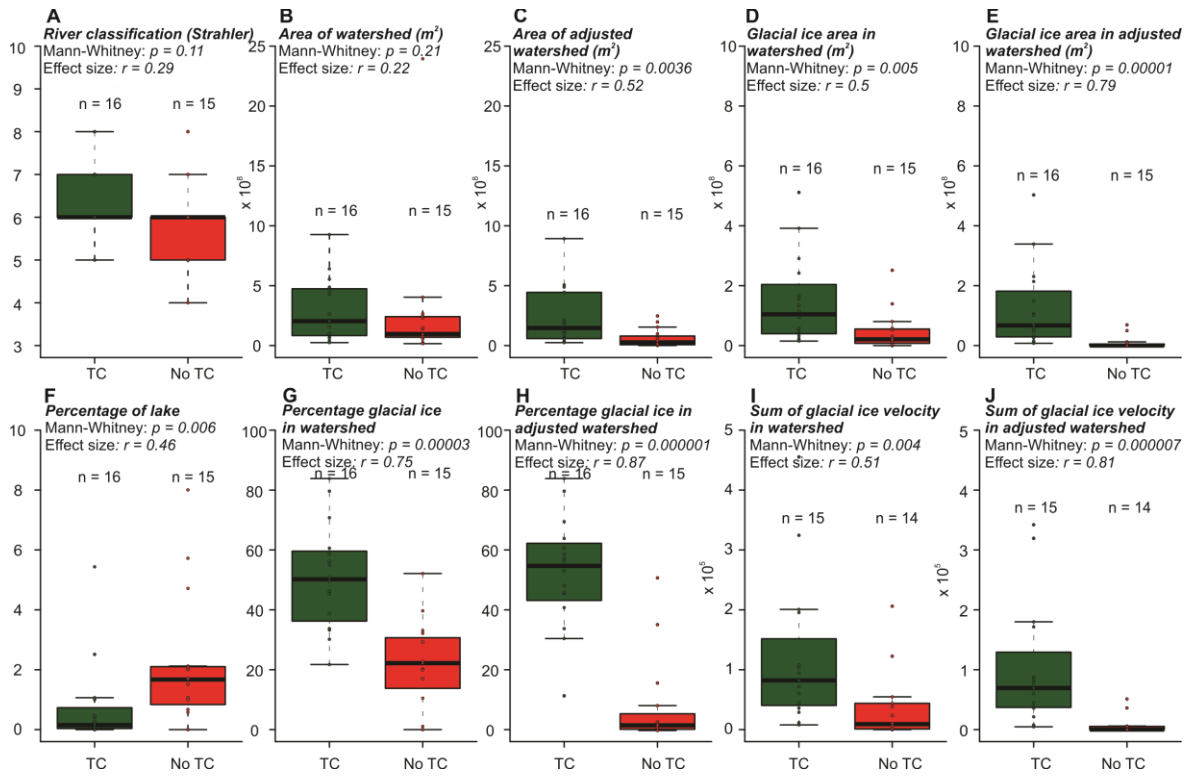
503

504 **Figure 3**



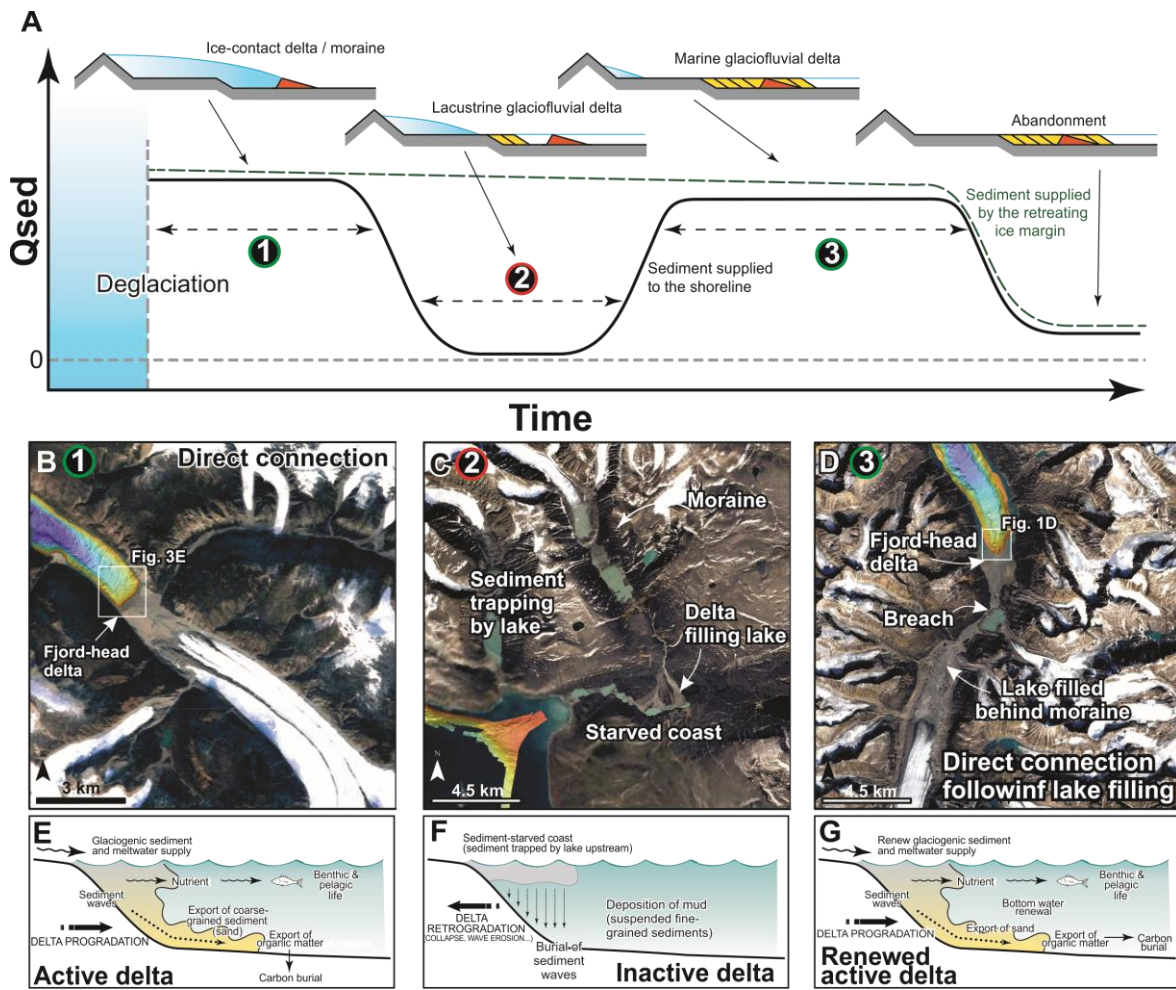
505

506 **Figure 4**



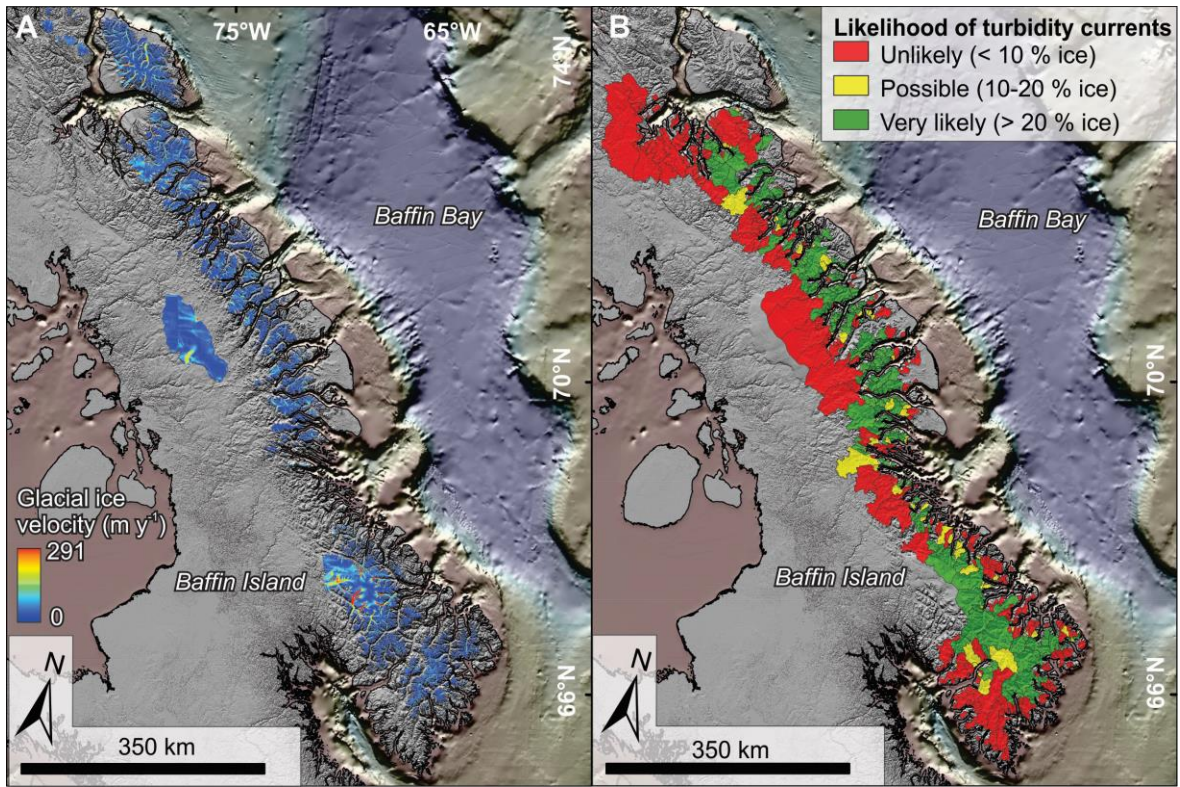
507

508 **Figure 5**



509

510 **Figure 6**



511